The Electrochemical Behaviors of Barrier-Type Anodic Films on Aluminum in Ammonium Adipate Solution

Han-Jun Oh[*] and Choong-Soo Chi[†]

Department of Materials Science, Hanseo University, Seosan 352-820, Korea
[†]School of Metallurgical and Materials Engineering, Kookmin University, Seoul 136-702, Korea
Received August 21, 1999

To investigate the effect of applied voltage and anodizing time on the formation and characteristics of barrier-type oxide layer, aluminum was anodized in 150 g/L ammonium adipate solution at 65 °C. The electrochemical behavior of oxide layers on aluminum was studied using impedance spectroscopy. The fitted results of impedance spectroscopy show clearly that the thickness of the oxide film subjected to applied anodic voltage increased linearly at a ratio of 1.42 nm/V, but the effect of the anodizing duration at constant voltage on film thickness was not remarkable. From a comparison of the fitting results and the observed microstructure using TEM, the fitted capacity by equivalent circuit can be directly converted to an oxide thickness.

Introduction

The barrier-type anodic oxide layer on aluminum are used as a dielectric layer in aluminum electrolytic capacitors and the electrical properties of capacitors depending on the dielectric characteristics and dimensions of anodic oxide film in relation to the electrochemical oxidation process for film formation. Thus, it is important in the manufacture of electrolytic capacitor to form anodic oxide films with dielectric properties for high performance. The formation of barrier-type oxide film on aluminum has been reported by many authors,[1-4] but there have been few reports that mention the electrochemical behaviors of barrier-type oxide film formed directly in ammonium adipate solution. In this study, the influence of anodizing time and applied voltage on the formation of anodic film in ammonium adipate solution are investigated. Also the formation rate and the dielectric properties of barrier-type anodic films are examined. For the evaluation of the properties of barrier-type anodic films in this paper electrochemical impedance spectroscopy (EIS) was applied. In general the oxide films on Al, Ti, Nb and Ta have a variable stoichiometry[5-7] with gradual reduction of oxygen deficiency towards the oxide-electrolyte interface. Therefore, the impedance properties of a barrier-type oxide layer on aluminum have not been fully described with an equivalent circuit of a simple RC element for an ideal capacitor. Thus, for the interpretation of impedance spectra for oxide layers of inhomogeneous dielectric, the Young impedance,[8] which differ from the behavior of ideal capacitors, was introduced. In this paper for comparison with the oxide thickness evaluated by impedance spectroscopy, the thickness of the barrier-type anodic film is examined by the transmission electron microscopy (TEM) and the Rutherford backscattering spectroscopy (RBS).

Experimental Section

Oxide film formations. A sheet of aluminum (99.99 wt%, Tokai Metals Co, Japan) for oxide layer was electropolished in a perchloric acid/methanol mixture at 20 V for 5 min. at 5 °C, then washed in distilled water and finally dried in a cool air stream. After electropolishing, the aluminum oxide films were prepared at a constant voltage of 140 V for 5, 10, 15 and 20 min in electrolyte. And for analysis of the effect of anode voltage on film thickness the samples were anodized at 80, 100, 120 and 140 V in electrolyte for 10 min. Anodizing was accomplished with the 150 g/L ammonium adipate ($NH_4OCO(CH_2)_4COONH_4$) solution at 65 °C. The anodic process in ammonium adipate solution formed the barrier-type oxide films. The anodic film thickness formed on aluminum differed according to applied potential and duration time.

After anodizing, the oxide layers were washed and rinsed in distilled water and were prepared for working electrode. The behavior of these oxide films was studied by impedance spectroscopy at 25 °C in 0.5 M K_2SO_4, an unstirred and aerated solution. All potentials are referenced to the Hg/Hg_2SO_4 /0.5 M K_2SO_4 solution in this paper. A platinum sheet was used for the counter electrode. The exposed total area of the working electrodes in electrolyte was 1 cm^2.

Impedance spectroscopy measurements. Electrochemical impedance spectroscopy experiments were performed using commercially available equipment (IM6, Zahner-electric, Germany). The computer system integrated into this device was used for measurement and data evaluation. All impedance spectra were plotted against the frequency range. The impedance spectra were measured at open-circuit potential imposing a low amplitude AC voltage signal of 10mV. The total complex impedance of the material electrode system is recorded as a function of the applied frequency.

The recorded impedance spectra are treated by

$$\ln\{Z(\omega)\} = \ln\{|Z(\omega)|\} + i\varphi(\omega)$$
$$\text{or } \log\{Z(\omega)\} = \log\{|Z(\omega)|\} + i\varphi(\omega)\log e \quad (1)$$

Since the real part of log Z according to Eq. (1) is the logarithm of modulus $|Z|$ and the imaginary part is the phase angle φ, it is obvious that Bode diagrams ($\log|Z|$ *vs.* $\log f$, φ *vs.* $\log f$) should be used if frequency dependencies are to be

explicitly be represented. The advantages of Bode plots and the loss of information resulting from Nyquist plots were convincingly demonstrated by Mansfeld.[9] After the measurement of the complex impedance as a function of frequency the electrochemical behavior of the oxide layer on aluminum can be analyzed with fitting of equivalent circuit. This is performed by a computer simulation and fitting program.[10,11]

Transmission electron microscopy. In order to compare the oxide film thickness with the value calculated from impedance spectroscopy and investigate the microstructures, the cross sections of the aluminum substrate and its attached aluminum oxide layer were examined by transmission electron microscopy (TEM). For ultramicrotomy, a narrow strip of the anodized specimen was embedded with a mixture of epoxy resin and a hardener. After curing at 60 °C for 24 hours, the specimen was sliced into thin sections of about 20-25 nm in thickness with a diamond knife. The slicing direction of the cutting edge of the diamond knife with respect to sample holder was perpendicular to the interface plane between the substrate and the oxide film in order to minimize compressive-tensile stresses in the direction of thickness measurement. The sectioned specimens, which were floated on a pool of distilled water contained in the knife assembly, were picked up on copper grids and observed at accelerating voltage of 100 kV, using transmission electron microscope (JEM 1210).

Rutherford backscattering spectroscopy. The RBS measurements were carried out by irradiating with $4He^{2+}$ at 2 MeV, using a tandem-type accelerator (6SDH-2 Pelletron). The scattered particles were detected at a 170° scattering angle to the incident beam direction normal to the oxide film on aluminum substrate. The energy distributions of the scattered ions were accumulated in 1024 channel spectra.

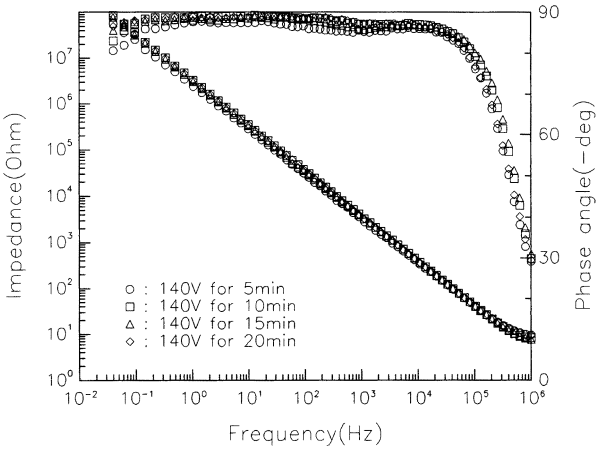

Figure 1. Bode diagram of the measured impedance spectra on anodic oxide layer formed at 140V for 5, 10, 15 and 20 min in ammonium adipate solution.

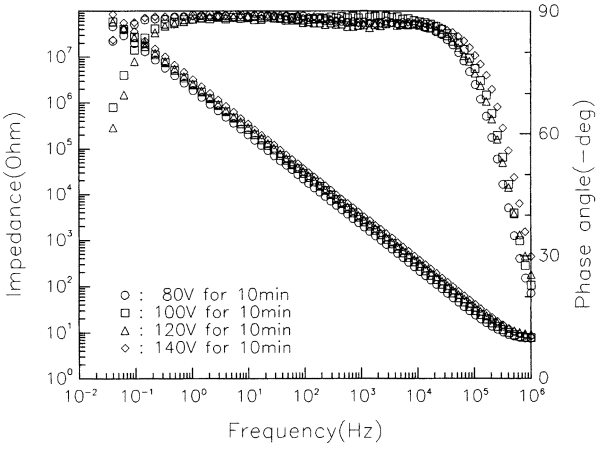

Figure 2. Bode diagram of the measured impedance spectra on anodic oxide layer formed for 10 min at 80V, 100V, 120 and 140V in ammonium adipate solution.

Results and Discussion

Impedance spectroscopy. When aluminum is anodically oxidized at constant potential, the currenttime response during oxide film growth on the aluminum can provide information regarding the type of film that is being formed. For a compact barrier film growth,[1,4] the current-time response shows that a rapidly decaying current leads to small steady state values, and after a short time the anodic current slowly and continuously decreases with time. Eventually a steady state is reached. At this stage the steady-state current is generally related to the rate of electrochemical dissolution of metals through the passive film and the chemical dissolution of the oxide and the rate of film growth can be characterized. In this paper, the impedance measurements for an analysis of the effect of anodizing time on anodic film properties were carried out after a short period of stabilization. To investigate the formation of anodic film, the anodic films were produced not only at 140 V for 5, 10, 15 and 20 min but also at 80, 100, 120 and 140 V for 10 min in 65 °C ammonium adipate solution.

The measured impedance spectra of anodic films are shown in Figures 1 and 2. The spectra of anodic films on pure aluminum were recorded at open-circuit potential in the frequency range from f_{min} = 10 MHz to f_{max} = 1 MHz. In the measured spectra, the impedance behavior represents passive oxide layer characteristics, of which capacitive response is illustrated by a phase angle close to -90° over a wide frequency range. Figures 1 and 2 show no significant differences between their impedance behavior.

Equivalent circuit. To evaluate the measured impedance spectra, the simple equivalent circuit in Figure 3 was introduced. In the equivalent circuit, which consists of two impedance elements, oxide resistance and electrolyte resistance can be described in terms of resistance, and layer impedance in terms of Young impedance. In general, the anodic oxide films on aluminum are characterized by variable stoichiometry, with gradual reduction of oxygen deficiency towards the oxide-electrolyte interface. In the case of anodic films on aluminum, because the properties of oxide layer have not been fully described with equivalent circuit of simple RC elements, Young impedance was utilized for data

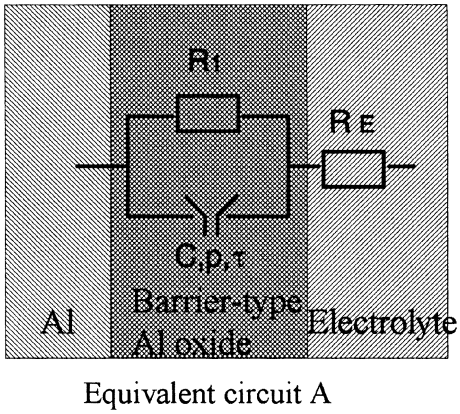

Figure 3. Electrical equivalent circuit A with Young impedance for fit of the oxide layer.

fitting instead of an ideal capacitor.

The physical meaning of Young impedance[8,12,13] is based on an oxide layer with behavior of non-ideal capacitor. The oxide layer is properly described by a dielectric layer of surface area A, thickness d and dielectric constant ε with a vertical decay of conductivity

$$\sigma_{Y(x)} = \sigma_{Y(x=0)} [1-\exp(-x/d_0)] \quad (2)$$

in an outer zone of effective thickness d_0, at a distance x from the surface.

Its impedance depends on three parameters: capacitance C_Y, relative penetration depth p and time constant τ, according to the following expression,

$$Z_Y = \frac{p}{i\omega C_Y} \ln\left(\frac{1 + i\omega\tau \exp(p^{-1})}{1 + i\omega\tau}\right) \quad (3)$$

where $C_Y = \varepsilon_o \varepsilon A/d$, $p = d_0/d$, $\tau = \varepsilon_o \varepsilon(0)/\sigma(0)$. (4)

In these equations C_Y is the capacitance of the oxide layer, ε is the dielectric constant for aluminum oxide, ε_o is the permittivity of free space ($\varepsilon_o = 8.85\times10^{-12}$F/m), A is the surface area, d is the thickness of oxide, and $\sigma(0)$ is the conductivity at metal-oxide interface.

In the dielectric of the capacitor with a vertical gradient of the conduction in the direction x (distance from metal/oxide interface to surface), the local time constant $\tau(x)$ at a distance x from the surface depends only on the local dielectric constant $\varepsilon(x)$ and the local conductivity $\sigma(x)$ according to

$$\tau(x) = \varepsilon_o \varepsilon(x)/\sigma(x), \quad (5)$$

which increases from outside to inside. At the metal/oxide interface (x=0), according to Eq. (5), the time constant represent $\tau = \varepsilon_o \varepsilon(0)/\sigma(0)$ in Eq. (4). If $p(=d_0/d)$ is the relative penetration depth of the conduction in the layer of the total thickness d, then σ at $x = d_0$ is decayed to $\sigma(d_0) = \sigma(0)/e$.

These behaviors of Young impedance are presented as Bode plots in Figure 4, and it can be clearly seen that Young impedance converges with decreasing frequency asymptotically to a resistance[8,10] by Eq. (3)

$$\lim_{\omega \to 0} Z_Y = R_Y = \frac{\tau p}{C_Y}(\exp(1/p)-1) \quad (6)$$

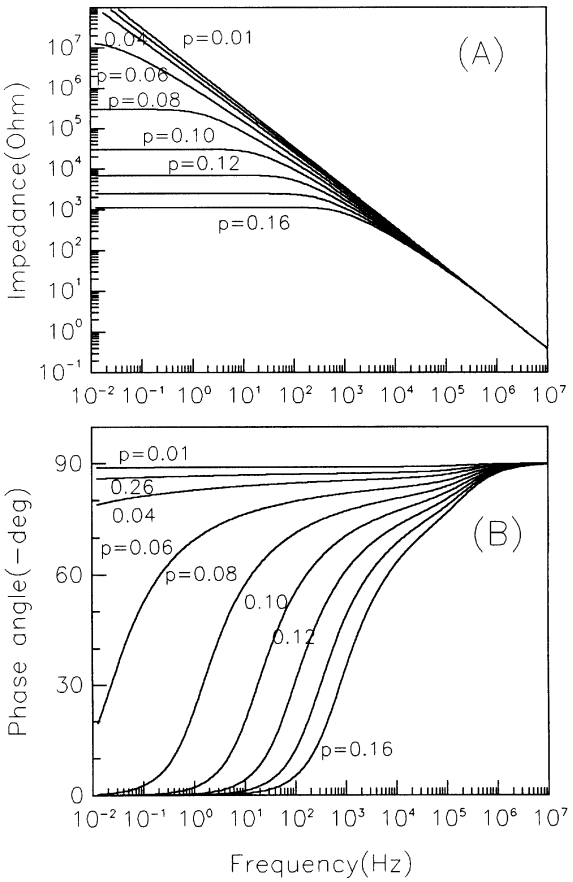

Figure 4. Impedance spectra of non ideal capacitance according to Young model. The impedance and phase shift angle depend on parameter p at C_Y=41nF/cm^2 and τ=572ns, which is fitted element from spectrum measured on anodic film formed at 140V for 5 min.

and with increasing frequency to a capacitance.

$$\lim_{\omega \to \infty} Z_Y = \frac{1}{i\omega C} \quad (7)$$

The impedance characteristics in Figure 4 depend on parameter p, the relative penetration depth, which is depends on the effective range between the charge carrier concentration and oxide thickness. If p is small, *i.e.*, it can be associated with the rapid decrease of carrier concentration density or the relatively large thickness of the oxide layer, in these cases, the Young impedance for the fit is especially valid. If p is zero, Young impedance behaves like an ideal capacitor.

Therefore, the impedance magnitude of circuit model A in Figure 3, according to the discussion above, can be determined by the frequency range. At very low frequencies, the circuit impedance, according to Eq. (6), is given Eq. (8).

$$Z_A = R_E + (R_Y^{-1} + R_1^{-1})^{-1} \quad (8)$$

But at high frequencies range, the circuit impedance, according to Eq. (7), can be described by Eq. (9).

$$Z_A = R_E + \frac{R_1}{1 + (2\pi f \cdot R_1 \cdot C_Y)^2} - \frac{i2\pi f \cdot R_1^2 \cdot C_Y}{1 + (2\pi f \cdot R_1 \cdot C_Y)^2} \quad (9)$$

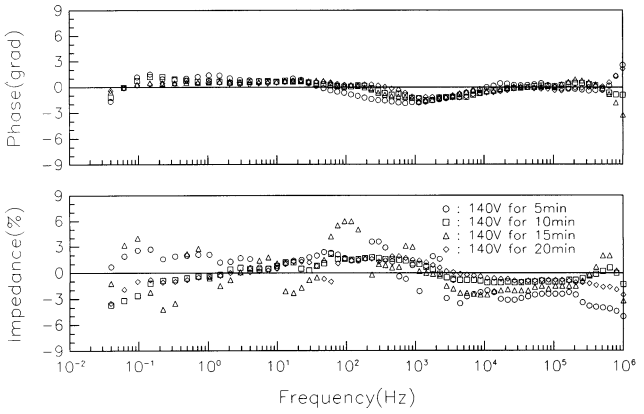

Figure 5. Deviation plots for fitting of the spectra measured on anodic film formed at 140V at 5 min, 10 min, 15 min and 20 min with equivalent circuit A.

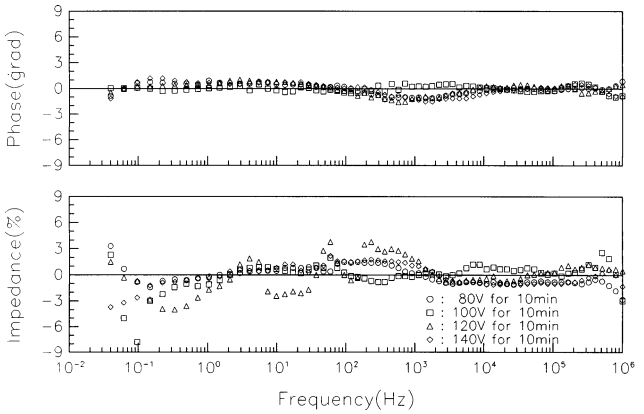

Figure 6. Deviation plots for fitting of the spectra measured on anodic film formed at 80V, 100V, 120V and 140V for 10 min with equivalent circuit A.

Deviations of fitted values. The quality of fitting to equivalent circuit is judged by the error distribution vs. the frequency, comparing experimental with simulated data. Figures 5 and 6 show the deviations between the measured and fitted values of the impedance modulus (in dZ/Z, $(Z_{mea}-Z_{calc})/Z_{calc}\times100\%$) and phase angle (in $dW(grad)$, $W_{mea}-W_{calc}$) for each of the experimental frequency values. If the measured data agree with the assumed equivalent model, only random variations due to scatter of the experimental data are observed. If the measured data do not agree with the assumed equivalent model, a systematic trend, usually a sinusoidal variation, is observed.[14] Since no systematic errors and relatively small deviations in Figures 5 and 6 are observed, it can be assumed that the experimental data agree with the equivalent model. The fitted spectra evaluated in Figures 5 and 6 exhibit mean deviations of phase angle from 0.35° to 1.01° and from 1.54% to 4.83% for mean deviation of modulus of impedance from the measured ones.

These mean deviation plots show that the equivalent circuit A in Figure 3 is valid for analysis of the spectra.

The influence of anodizing time on anodic films. After the impedance spectra were fitted to circuit model A, the fit results of R_1 and C_Y were plotted vs. anodizing time at 140 V

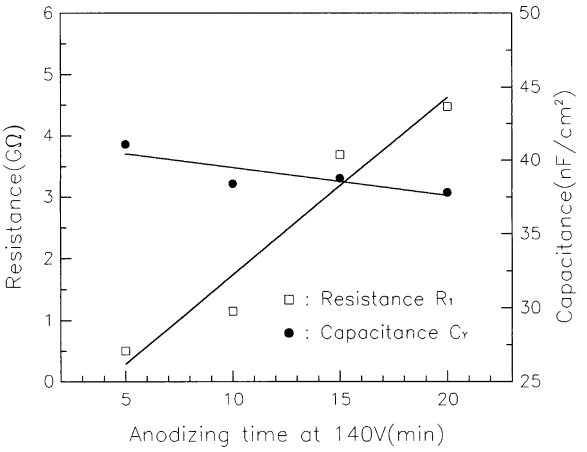

Figure 7. Oxide resistance and capacitance for the oxide films as a function of duration time at 140V.

in Figure 7. It shows the R_1, the bulk resistance of the barrier-type layer, vary in the range from several hundred MW to several GΩ, which is expected for a highly insulating material. In addition, C_Y, the layer capacitance of the barrier-type oxide, is relatively low and decreases slightly with anodic time. This slight decrease of C_Y may reflect the increase in the anodic film thickness with anodic time. In general, the calculated capacity C_Y can be directly converted to an oxide thickness.

From capacitance of oxide layer the anodic film thickness is calculated using the conventional equation, as given in

$$d_{ox} = \varepsilon\varepsilon_o Ar/C_Y \quad (10)$$

where d_{ox} is the thickness of the barrier-type oxide layer, C_Y is the capacitance of the Al_2O_3 layer, ε = dielectric constant for aluminum oxide, ε_o is the permittivity of free space (ε_o = 8.85×10^{-12} F/m), A is the surface area, r is the geometrical surface area factor. Taking ε = 8.5 for Al_2O_3[15] and r =1.05, the thickness of the oxide layer can be estimated. Figure 8 shows the relationship between anodic time vs. formed film thickness for a constant applied anodic voltage of 140V. In Figure 8, the effect of anodizing time on the film thickness is not so remarkable. The oxide films formed at applied constant anodic voltage of 140V indicate a thickness from 192 nm for 5 min. to 210 nm for 20 min. However, an early stage up to 5 min during anodization represents rapid film formation and growth. It is a reflection of a rapidly decaying current to small steady-state values in current-time response. At the stage of non-steady state current , the rate of film growth cannot be characterized

According to Habazaki,[16] the film with constant growth slope is formed as a result of the transport of ions across the film thickness in the presence of a high electric field. For anodizing of Al at high faradaic efficiency, it is established that about 40% of the film thickness is formed at the film-electrolyte interface by the migration of Al^{3+} ions outwards, while the 60% is formed at the metal-film interface by the migration of O^{2-}/OH^- ions inwards. Thus, the growth rate of anodic film in Figure 8 is proportional to a ratio of 0.97 nm/

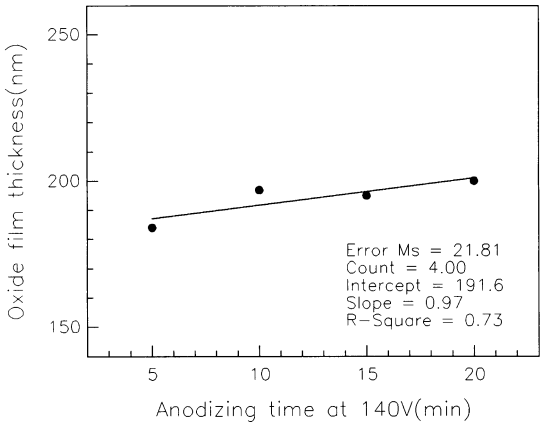

Figure 8. Thickness of the barrier-type oxide layer as a function of anodic duration time at 140V in ammonium adipate solution.

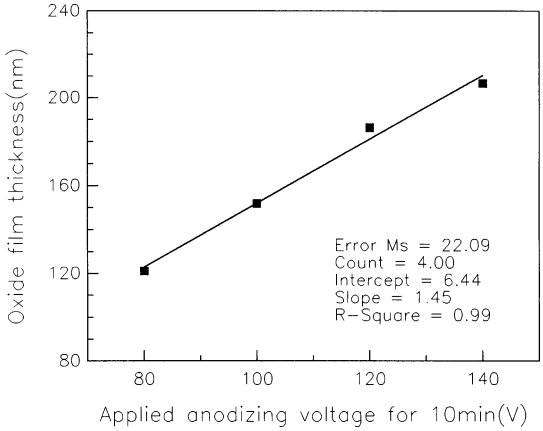

Figure 10. Thickness of the barrier-type oxide layer as a function of applied anodic voltage for 10 min in ammonium adipate solution.

min in ammonium adipate solution at the applied constant anodic voltage of 140 V.

The influence of applied voltage on anodic film. The fit results of R_1 and C_Y for barrier- type anodic film as a function of applied anodic voltage under constant time of 10 min are given in Figure 9. It can be seen from Figure 9 that the resistance of oxide film, R_1, increases from 570 MΩ to 1.15 GΩ, while C_Y gradually decreases from 65.6 nF/cm^2 to 38.6 nF/cm^2 with increasing anodic voltage. From the capacitance of the oxide layer the thickness of the anodic film can be calculated by the Eq. (10). Figure 10 shows the thickness of anodic film as a function of applied anodic voltage for 10 min in ammonium adipate solution. For an anodizing time of 10 min the anodic film thickness increases from 120 nm at applied voltage of 80 V to 205 nm at 140 V. Figure 10 indicates that the anodic film thickness is dependent on anodic voltage with a ratio of 1.45 nm/V in ammonium adipate solution at anodic voltage range of 80 to 140 V for 10 min. This growth ratio of oxide film is similar to the results obtained by Takahashi,[17,18] who reported a thickness/voltage ratio of 1.42 nm/V for the barrier oxide underlying the porous film formed on pure Al in neutral solution at 60 °C.

Comparison of the film thicknesses. In general, the fitted capacitance C_Y from impedance measurement can be directly converted to an oxide thickness by Eq. (10). To validate this concept, the oxide film thickness from impedance spectroscopy was compared with the value determined from transmission electron microscopy (TEM) and Rutherford backscattering spectroscopy (RBS) on the barrier-type anodic film formed on pure aluminum in ammonium adipate at 140 V and 65 °C for 10 min.

Figure 11 shows a barrier-type oxide film with uniform thickness, for which the measured average values in thickness is about 200 nm. As can be seen the thickness observed under TEM correlates well with the thickness, 205 nm, determined by interpretation of impedance spectroscopy. Although the calculated film thickness from impedance specroscopy is 2.5% thicker than that obtained by TEM, the validity of the interpretation by impedance spectroscopy can be confirmed by the direct observation of the film thickness using TEM.

Figure 12 shows the cross section of the oxide as Figure 11. However, the morphology of the layer is different from

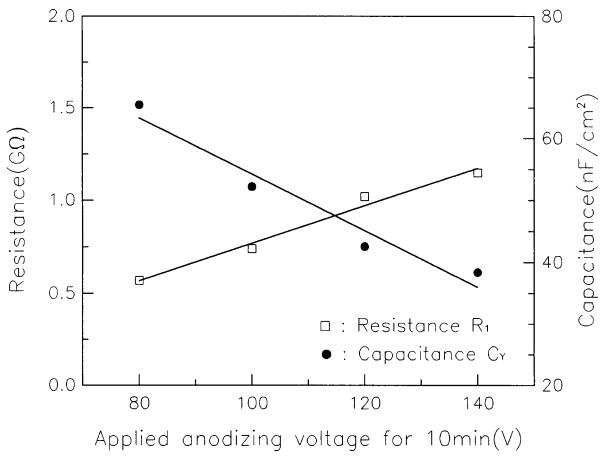

Figure 9. Oxide resistance and capacitance for the anodic films as a function of anodic voltage for 10 min.

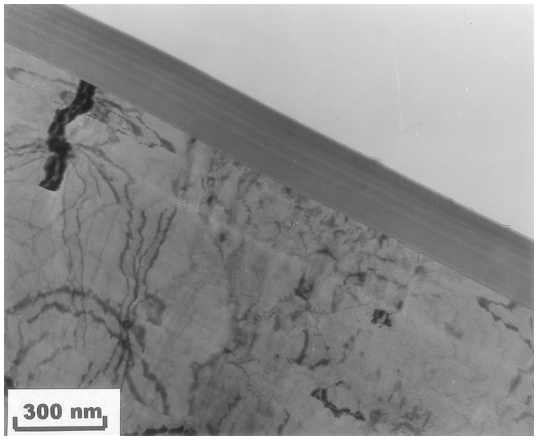

Figure 11. Transmission electron micrograph of the cross section of the barrier-type oxide film formed on pure aluminum in ammonium adipate at 140V and 65 °C for 10 min.

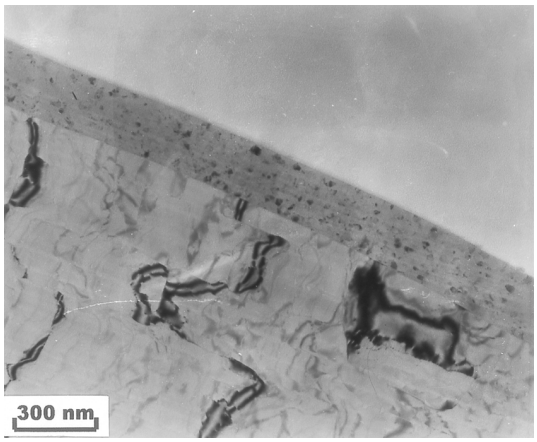

Figure 12. Transmission electron micrograph as Figure 11, but after electron-beam induced crystallization of the amorphous oxide films.

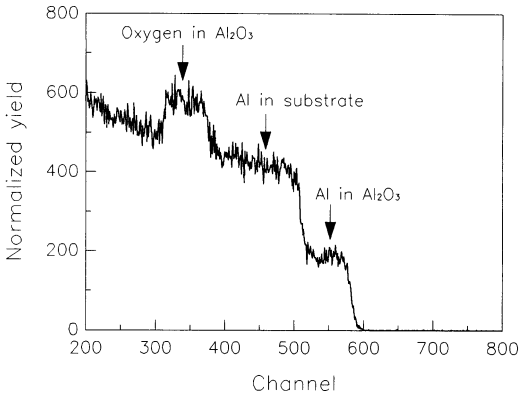

Figure 13. Rutherford backscattering spectroscopy result on the barrier type anodic film formed on pure aluminum in ammonium adipate at 140V and 65 °C for 10 min.

that of the film in the structure. It is implied that the anodic oxide film is formed in amorphous state during anodization, which has been transformed into the crystalline state by electron-beam irradiation for several ten second periods.

Rutherford backscattering spectroscopy. Figure 13 shows the backscattering spectrum from an anodic film formed on aluminum in ammonium adipate solution at 140 V for 10 min. The spectrum shows that the profiles from the elements of aluminum and oxygen in the oxide films are superimposed on the background profile scattered from the aluminum substrate beneath the film. Aluminum and oxygen elements corresponding to the scattering energies from the film surface are shown in the profile.

It can be calculated that the anodic film has a composition almost equivalent to Al_2O_3, using the Bragg's rule,[19] and a thickness value of 192 nm, assuming that the density[20] of the barrier-type anodic oxide film for the amorphous state is 3.10 g/cm^3. While the density of α-Al_2O_3 (corundum) is nearly 4.0 g/cm^3, the density of γ-Al_2O_3 is usually close to 3.2 g/cm^3, in spite of the fact that both of the compounds possess same nominal stoichiometry. Thus, although as-formed oxide film has a similar ratio to that of the stoichiometric aluminum oxide compounds in the number of alumimum and oxygen atoms, this does not mean that the film is crystalline. As can be seen in Figure 12, where the amorphous oxide layer goes through electron-beam induced crystallization, it is noteworthy merely that the elements of aluminum and oxygen are present in this proportion.

Conclusion

The effect of applied voltage and anodizing time on the formation and characteristics of the barrier-type oxide layer was investigated by electrochemical impedance spectroscopy. Because the barrier-type anodic films exhibit a non-ideal capacitive behavior, the Young impedance is a very useful element for the characterization of aluminum oxide layer in an equivalent circuit.

From a comparison of the fitting results with both the observation of microstructure by TEM and the interpretation of RBS, the fitted capacitance by the equivalent circuit can be directly converted to the oxide thickness. The fitted results used by Young impedance show clearly that the thickness of oxide film with applied anodic voltage increased linearly with a ratio of 1.45 nm/V, and in the case of the effect of the anodizing duration at a constant 140 V on film thickness, the thickness increased with a ratio of 0.97 nm/min.

In terms of the number of aluminum and oxygen atoms, as-formed oxide film has a similar ratio to that of stoichiometric aluminum oxide compounds, but the structure of the film is amorphous and can be transformed into crystal by electron-beam irradiation.

The electrochemical behavior of anodic film and the growth rate of barrier-type oxide layer formed in ammonium adipate solution can be monitored by electrochemical impedance spectroscopy.

Acknowledgment. The authors thank Dr. Yong-soo Jeong at the Korea Institute of Machinery and Metals for his contribution and helpful advice.

References

1. Thomas, S. C.; Birss, V. I. *J.Electrochem. Soc*. **1997**, *144*, 3377.
2. De Laet, J.; Terryn, H.; Vereecken, J. *Electrochim. Acta* **1996**, *41*, 1155.
3. Li, Y.; Shimada, H.; Sakairi, M.; Shigyo, K.; Takahashi, H.; Seo, M. *J. Electrochem. Soc*. **1997**, *144*, 866
4. Gudic, S.; Radosevic, J.; Kliskic, M. *J. Appl. Electrochem.* **1996**, *26*, 1027.
5. Grundner, M.; Halbritter, J. *J. Appl. Phys.* **1980**, *51*, 397.
6. Gray, K. E. *Appl. Phys. Lett.* **1975**, *27*, 462.
7. Göhr, H.; Schaller, J.; Schiller, C.-A. *Electrochim. Acta* **1993**, *38*, 1961.
8. Göhr, H.; Oh, H-J.; Schiller, C.-A. *GDCh-Monographie Band 2* **1995**, 341.
9. Mansfeld, F. *Corrosion Science* **1988**, *44*(8), p 558.
10. Göhr, H. *Ber. Bunsenges. Phys. Chem.* **1981**, *85*, 274.
11. Göhr, H. *Z. Physik. Chem. N. F.* **1986**, *148*, 105.

12. Young, L. *Anodic Oxide Films*; Academic Press: New York, 1961; p 253-267.
13. Young, L. *Faraday Soc.* **1955**, *51*, 1250.
14. Mansfeld, M.; Shih, H.; Greene, H.; Tsai, C. H. *Electrochemical Impedance: Analysis and Interpretation*; ASTM. Philadelphia, 1993; p 37-53.
15. Kuznetsova, A.; Burleigh, T. D.; Zhukov, V.; Blachere, J.; Yates, Jr. J. T. *Langmuir* **1998**, *14*(9), 2502.
16. Habazaki, H.; Skeldon, P.; Thompson, G. E.; Wood, G. C. *Philos. Mag. B* **1995**, *71*, 81.
17. Takahashi, H.; Nagayama, M. *Electrochim. Acta* **1978**, *23*, 279.
18. Takahashi, H.; Nagayama, M. *Corros. Sci.* **1978**, *18*, 911.
19. Feldman, L. C.; Mayer, J. W. *Fundamentals of Surface and Thin Film Analysis*; North-Holland: 1986; p 47-51.
20. Skeldon, P.; Shimizu, K.; Thompson, G. E.; Wood, G. C. *Surf. Interface Anal.* **1983**, *5*, 247.